SWIFT-XRT-CALDB-04

Release Date: April 7th, 2009

Prepared by: Andrew Beardmore, Tony Abbey, Olivier Godet (UL), Claudio Pagani (PSU), Matteo Perri, Milvia Capalbi (ASDC)

Date revised: April 7th, 2009

Revision: 9.0

Revised by: Andrew Beardmore

SWIFT-XRT CALDB Rev 9.0 Release Note

SWIFT-XRT-CALDB-04: Gain

1 Component Files

Table 1: Latest CALDB component files.

FILENAME	VALID DATE	RELEASE DATE
swxpcgains0_20010101v008.fits[a]	01-Jan-2001	07-Apr-2009
swxwtgains0_20010101v009.fits[a]	01-Jan-2001	07-Apr-2009
swxpdgains0_20010101v008.fits[a]	01-Jan-2001	07-Apr-2009
swxpcgains6_20010101v008.fits[b]	01-Jan-2001	07-Apr-2009
swxwtgains6_20010101v009.fits[b]	01-Jan-2001	07-Apr-2009

[a] 's0' refers to substrate voltage (V_{ss}) 0 V gain files.

[b] 's6' refers to $V_{ss} = 6$ V gain files. The substrate voltage was raised permanently to this value on 2007-Aug-30 at 14:25UT.

2 Introduction

This document contains a description of the gain calibration analysis performed at Penn State and Leicester University to produce the gain calibration products for the *Swift*-XRT Calibration Database (CALDB).

Swift Software version 3.2, released on 2009-Apr-07, included preliminary changes to the XRT analysis task XRTCALCPI which required a modified gain file format. As a consqeuence, both substrate voltage 0 V and 6 V gain files have been released this time, to accomodate the new format, though the gain coefficients have only been updated in the 6 V files (see below).

3 Changes in Gain File release (revision 9)

The loss of the CCD active cooling system shortly after launch forced the instrument to rely on passive cooling provided by the XRT radiator in order to operate the detector in the -75°C to -50°C temperature range rather than the -100°C envisaged before launch. The main effect of operating at such temperatures is a significant level of dark current and elevated CCD noise at low energies, with an increasing number of hot and 'flickering' pixels at higher temperatures.

On 2007-Aug-30 at 14:25UT, the XRT team performed a planned substrate voltage (V_{ss}) change from 0 V to 6 V in order to reduce the thermally induced dark current when the operating temperature is above -55 °C. Prior to the change, preliminary observations of Cas A and the Crab at a V_{ss} of 6 V showed a reduction in the Quantum Efficiency of the order of 10% at 6 keV (Godet et al. 2007, SPIE, 6686) and an increase of about 5% in the gain due to the change in the gain of the output FET. The latter meant separate gain files are needed depending on the substrate voltage at the time of a given observation. The files are distiguished using the notation *s0* (for $V_{ss} = 0$ V) and *s6* (for $V_{ss} = 6$ V) in their respective file names. The *Swift* software tools were updated to perform a query for the relevant gain file to be used depending on the substrate voltage setting. The previous release of the gain files (v007 & v008) included simple placeholder estimates of the gain file parameters for the $V_{ss} = 6$ V operation based on the earlier, preliminary calibration observations. This release updates those files.

In addition to the substrate voltage change, in 2008 June, after successful XRT flight software updates, the XRT CCD began permanently operating in full frame mode ('pcw3'), whereby the entire 600×600 imaging area of the CCD is read out. This has enabled us to continuously collect corner source ^{55}Fe calibration data (see figure A.1) when operating in photon counting mode and has provided us with a wealth of information on the gain and charge transfer efficiency (CTE) behaviour as a function of time and CCD temperature since this time.

The latest CALDB release (2009-Apr-07) includes new versions of the $V_{ss} = 6$ V gain files, with improved gain coefficients, for both Photon Counting (PC) mode (**swxpcgains6_20010101-v008.fits**) and Windowed Timing (WT) mode (**swxwtgains6_20010101v009.fits**).

The $V_{ss} = 0$ V gain file coefficients have not been changed for this release, so the previous calibration documents (SWIFT-XRT-CALDB-04_v8 and SWIFT-XRT-CALDB-04_v2) still describe the construction of the $V_{ss} = 0$ V gain files.

However, it was necessary to update the $V_{ss} = 0$ V gain file version numbers as well, as the gain

file format (and hence the software tools) have been modified to introduce new parameters (i.e. FITS-file table columns) in preparation for a future CALDB release that will have the capability to correct for the effects of the largest charge traps which have developed on the CCD. This feature is presently disabled (by virtue of the fact that no traps are identified in the current gain files) while it undergoes testing (see section 5).

4 Gain file creation

4.1 Gain and CTI measurements

The corner source data were reprocessed to ensure the latest photon counting mode bias corrections were applied, as this has previously been shown to correct the gain during the times of highest CCD operating temperatures (above -55°C) and is the default operation for the *Swift* software tools. Grade 0 PHA spectra were extracted from each of the corner sources as a function of time and CCD temperature. The spectra near the ^{55}Fe line were then fit with the following asymmetric gaussian function :

$$\begin{aligned} G(x) &= N \exp\left(-0.5\left(\frac{x-x_c}{\sigma_1}\right)^2\right) \qquad (x < x_c) \\ &= N \exp\left(-0.5\left(\frac{x-x_c}{\sigma_2}\right)^2\right) \qquad (x > x_c) \end{aligned}$$

where x_c is the line centre, σ_1 the line width for $x < x_c$, σ_2 the line width for $x > x_c$, and N the normalisation. This models the line profile better and returns more accurate line centroids than a simple gaussian, as the effect of CTI is to broaden the low energy line wing significantly more than the high energy line wing (Godet et al. 2009, A&A, 494, 775).

The formulation behind the derivation of the gain file coefficients from the measured line centroids is given in appendix A. Figure 1 illustrates the measured line centroids, gain and CTI coefficients from 2007-Sep-05 to 2009-Jan-31 at a CCD temperature of -57°C.

Due to the excellent quantity and statistical quality of the corner source data obtained since 2008-June we have been able to study and quantify the measured gain and CTI coefficients behaviour as a function of time and CCD temperature. Figure 2 shows the gain (GC0) and CTI coefficients (GC1,2) plotted as a function of CCD temperature at 4 representative epochs. The data reveal the gain has evolved to become less sensitive to the CCD temperature, while the parallel CTI decreases with increasing temperature whereas the serial CTI increases slightly with temperature.

We have parameterised the gain and CTI time (t) and CCD temperature (T) dependence using the following functional form :

$$z(t,T) = a + b\,t + c\,T + d\,t^2 + e\,T^2 + f\,t\,T.$$

The model curves are shown plotted with the data in figure 2.

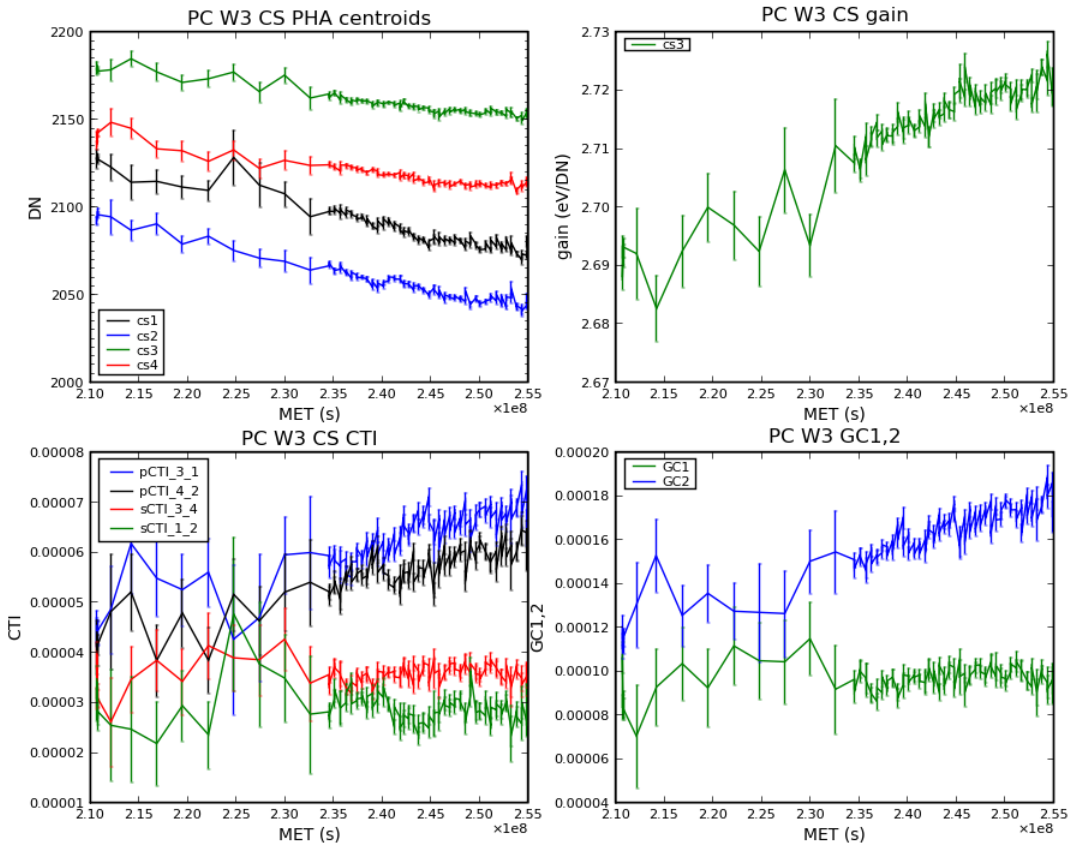

Figure 1: *Swift*-XRT CCD gain and CTI measurements from the corner source data at a CCD temperature of -57°C from 2007-Sep-05 to 2009-Jan-31. The top-left panel shows the measured ^{55}Fe line centroids. The top-right panel shows the gain coefficient ($GC0$) estimated using equation A.11. The bottom-left panel shows the measured CTI coefficients for the 4 pairs of corner sources. The bottom-right panel shows the estimated gain file $GC1$ (serial) and $GC2$ (parallel) coefficients. (Error bars are 1σ estimates.)

The parameterised GC0, GC1 and GC2 (see equation A.12) values were then converted into a template gain file with coefficients calculated at monthly intervals and at three discrete temperatures (-73, -60.5, -48°C). The *Swift*-XRT software task XRTCALPI interpolates over time and temperature when applying the gain calculation to the event data.

The template gain file was tested on various data sets which included the corner source data (PC mode) and the line rich SNRs E0102 and Cas A (both PC and WT mode). The low energy spectrum of SNR E0102, in particular, is sensitive to the presence of residual offsets in the energy scale.

PC mode observations of E0102 taken during 2007-Sep-25 to 2007-Oct-02 and 2008-Oct-01 to 2008-Oct-04 revealed the need for an additional offset of 15 eV. A similar level of offset was obtained from PC mode observations of Cas A taken on 2007-Oct-05 and 2008-Sep-04.

At present, we have no independent measure of the CTI characterisation in WT mode so use the PC mode CTI coefficients in the construction of the WT gain file. Like PC mode, we

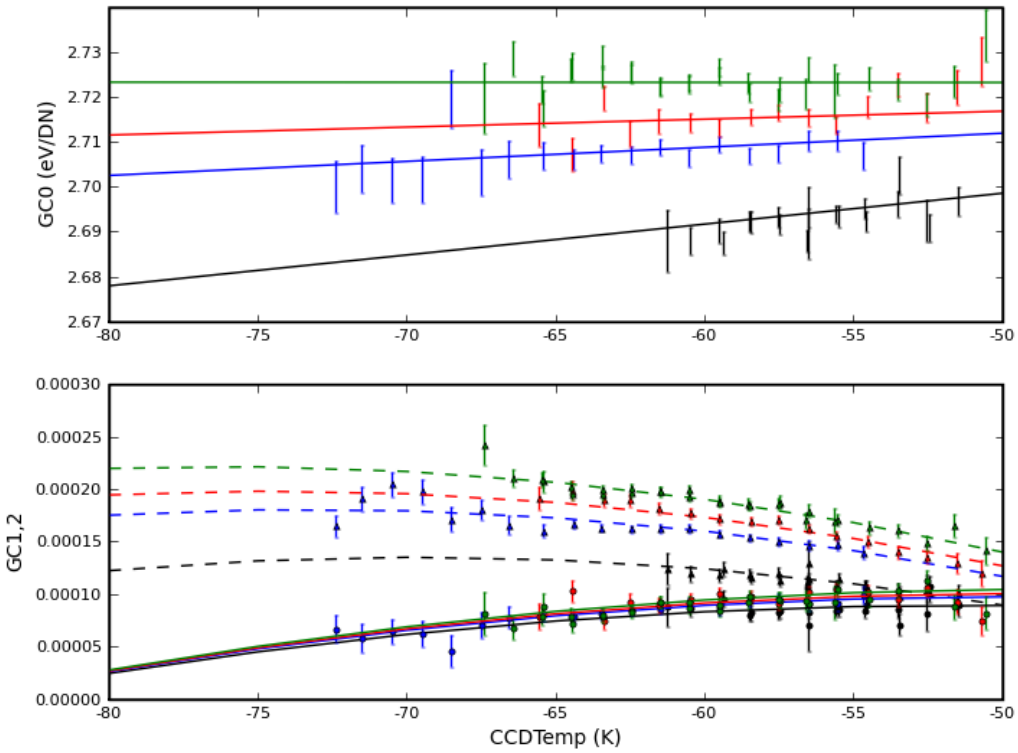

Figure 2: *Swift*-XRT CCD gain (GC0) and CTI (GC1,2) coefficients plotted against CCD temperature. The model described in the text is overplotted as the curved lines. For both panels the colour coding is a follows : black – 2007-Sep-06; blue – 2008-Jun-07; red – 2008-Sep-15; green – 2008-Jan-25. In the lower panel, the GC1 (serial) values are drawn as circles and the model is represented by the solid curves, while the GC2 (parallel) values are drawn as triangles and the model curves are shown dashed.

checked the residual offset using observations of E0102 taken in 2007-Sep-30 to 2007-Oct-01 and 2008-Aug-24 to 2008-Oct-09. These showed an average offset of 38 eV.

New substrate voltage 6V gain files for PC and WT mode were created from the template gain file with the appropriate offsets measured above included as the GC3 coefficient (see equation A.12). The files are named **swxpcgains6_20010101v008.fits** and **swxwtgains6_20010101v009.fits**.

4.2 Quality of the new gain files

The new gain files offer a big improvement over the previous substrate voltage 6 V release in that they track the evolving CTI and gain with greater accuracy then before. However, some limitations remain.

By testing the new v008 PC gain file on the corner source data, the following mean centroids (standard deviations in brackets) were obtained (in keV) over the time interval from 2007-Sep-01 to 2009-Jan-31: CS1 – 5.880 (0.013), CS2 – 5.889 (0.014), CS3 – 5.895 (0.010), CS4 – 5.892

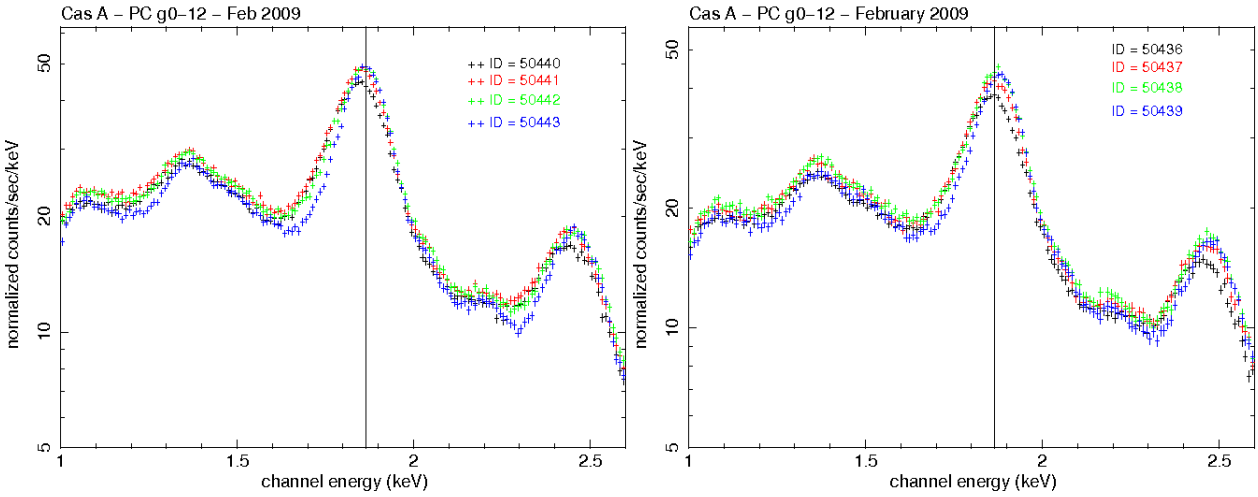

Figure 3: Photon counting mode Cas A observations taking in 2009-Feb at different locations on the CCD illustrating the good agreement in the recovered Si line energy (1.863 keV as measured by the XMM MOS for the entire remnant) as a function of source position using the new v008 gain file. The figure on the left shows observations with the remnant centre at DETX = 250 while the figure on the right shows the remnant centre placed at DETX = 350. The spectra are coloured according to the following DETY position : black - 450, red - 350, green - 250, blue - 150. The remnant has a size of 100 × 100 pixels as seen by the XRT. In general, the line centroids agree to ±10 eV.

(0.010). In particular, the CS3 results indicates an excellent agreement with the expected ^{55}Fe line energy (5.895 keV), though ∼ 10 eV variations are possible during individual observations.

Additionally, PC mode observations of Cas A placed at different detector positions were used to check the accuracy of the energy scale at the Si-Kα line (1.863 keV, when averaged over the SNR). As figure 3 shows, the Si-Kα line centroid is also recovered to an accuracy of ±10 eV, even when the source is observed at a large DETY position. (This figure also shows the worsening energy resolution for sources located at larger DETY positions.)

Like PC mode, the WT gain file offset was calibrated for sources observed near the centre of the CCD. For WT mode, however, observations of Cas A have revealed some residual offsets of $20 - 30$ eV at the Si-Kα line, which is larger when a source is located further away from the detector centre; especially so when outside the central 200 × 200 pixel region of the detector.

For typical astrophysical observations the effect of the residual offsets mentioned above will not be noticeable in XRT spectra due to their limited total counts. However, when bright, featureless continuum sources are observed any offset could become apparent near the instrumental edges of oxygen, silicon and gold, where dips or excesses up to $3 - 8$ percent might be visible in the fit residuals. The continuum spectral parameters derived from any spectral fitting procedure are generally not affected by such residuals within the limits of their derived statistical errors.

5 Expected updates

Radiation damage during the orbital lifetime of *Swift* continues to degrade the XRT CCD CTE, mostly through the production of charge traps. The PC mode gain and CTI coefficients are

continuously monitored using the ^{55}Fe calibration sources mounted at the 4 corners of the detector for in-flight calibration. The coefficients are updated in the gain files on a regular basis.

We are characterising the location and depth of the largest charge traps which have formed in the central regions of the CCD. By correcting for the most severe traps, we have shown that the FWHM of the detector can be significantly improved (e.g. Godet et al. 2009, A&A, 494, 775). While the XRTCALCPI task and gain-file format have been modified to perform such a trap correction, it is presently disabled in the current release as no traps are identified in the gain files. We expect to fully document this feature in a future release of the *Swift* software tools and CALDB once the traps have been identified and the trap correction procedure has been tested thoroughly.

Evidence from the corner source data, Cas A observations, and measurements of the nickel background line is accruing to suggest that the regular CTI correction should be energy dependent, which is presently not taken into account by the XRTCALCPI task. We aim to calibrate this energy dependence in the near future.

Finally, using observations of Cas A, along with theoretical modelling, we are investigating whether the CTI coefficients are significantly different in WT mode compared with PC mode.

APPENDIX

A SWIFT-XRT gain and CTI coefficient definitions

A.1 Introduction

The charge transfer efficiency (CTE) is defined as the fractional charge lossed per pixel during the charge transfer process. So after N transfers the remaining charge Q is

$$Q = Q_o(CTE)^N \tag{A.1}$$

where Q_o is the initial charge. Or in terms of charge transfer inefficiency $CTI = 1 - CTE$ this is just

$$Q = Q_o(1 - CTI)^N \tag{A.2}$$

A.2 Event energy measured in the SWIFT-XRT CCD22

A schematic of the *Swift*-XRT CCD22 is showed in figure A.1. When an incident X-ray of energy E is registered as an event at a detector position (X, Y) in the image section it suffers charge loss from Y transfers in the parallel direction through the image section, from $Y_S = 600$ transfers in the parallel direction through the frame-store section and from $X + 5$ transfers in the serial direction through the readout register (+5 as there are 5 additional pixels at the end of the readout register). In order to describe the total charge lost effectively we need separate CTI coefficients for the parallel transfer losses incurred in the image and frame-store sections

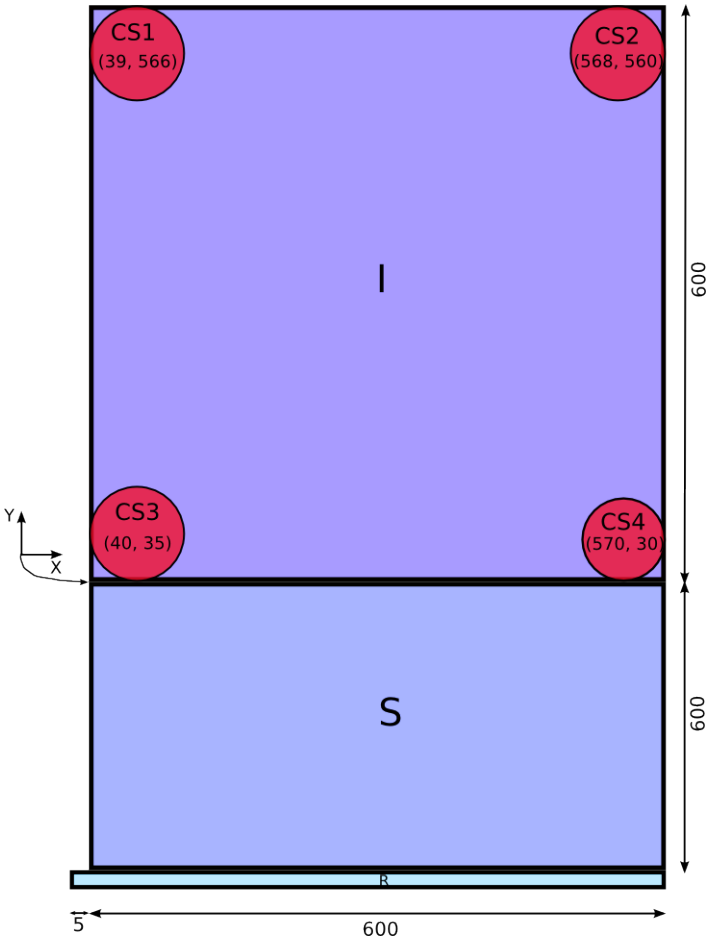

Figure A.1: Schematic of the *Swift*-XRT CCD22 identifying the imaging (I) and frame-store (S) sections, the readout register (R), and the ^{55}Fe corner sources (CS). Charged is clocked in the parallel direction through both the imaging and frame-store sections, which have charge transfer inefficiencies $CTI_{p,i}$ and $CTI_{p,f}$, respectively, and in the serial direction through the readout register with CTI_s.

($CTI_{p,i}$ and $CTI_{p,f}$, respectively, as the physical volume of the pixels are smaller in the latter compared with the former) and another for the serial transfer losses (CTI_s).

The event is registered by the ADC as a pulse-height analysed digital number D (i.e. the PHA value) according to the following:

$$D = \frac{E}{A}(1 - CTI_{p,i})^{Y}(1 - CTI_{p,f})^{Y_S}(1 - CTI_s)^{(X+5)} \tag{A.3}$$

Or rearranging slightly, this becomes

$$\begin{aligned} D &= E\left[\frac{(1 - CTI_{p,f})^{Y_S}(1 - CTI_s)^5}{A}\right](1 - CTI_{p,i})^{Y}(1 - CTI_s)^{X} \\ &= \frac{E}{A'}(1 - CTI_{p,i})^{Y}(1 - CTI_s)^{X} \end{aligned} \tag{A.4}$$

where $A' = A/((1 - CTI_{p,f})^{Y_S}(1 - CTI_s)^5$ and is the system gain, which accounts for the parallel charge transfer losses in the frame-store.

A.3 CTI coefficients

The parallel CTI can be determined from CS3 and CS1 by using equation A.4 to construct the ratio $(D_3 - D_1)/D_3$, where D_n are the measured ^{55}Fe central energies (in DN) for source $n = 1 \ldots 4$, which is

$$\begin{aligned} \frac{D_3 - D_1}{D_3} &= \frac{(1 - CTI_{p,i})^{Y_3}(1 - CTI_s)^{X_3} - (1 - CTI_{p,i})^{Y_1}(1 - CTI_s)^{X_1}}{(1 - CTI_{p,i})^{Y_3}(1 - CTI_s)^{X_3}} \\ &= 1 - (1 - CTI_{p,i})^{(Y_1 - Y_3)}(1 - CTI_s)^{(X_1 - X_3)} \quad \text{(A.5)} \\ &= 1 - (1 - CTI_{p,i})^{(Y_1 - Y_3)} \quad \text{(A.6)} \end{aligned}$$

where equation A.6 is a simplification assuming $X_1 \approx X_3$ for transfers dominating in the parallel direction (i.e. $Y_1 - Y_3 \gg X_1 - X_3$). Rearranging we find

$$CTI_{p,i} = 1 - \left(\frac{D_1}{D_3}\right)^{1/(Y_1 - Y_3)} \quad \text{(A.7)}$$

We often make use of the small number approximation (i.e. $(1 + x)^n \approx 1 + nx$) so equation A.6 becomes

$$\frac{D_3 - D_1}{D_3} = (Y_1 - Y_3)CTI_{p,i}$$

That is, the parallel CTI is

$$CTI_{p,i} = \frac{D_3 - D_1}{D_3(Y_1 - Y_3)} \quad \text{(A.8)}$$

A similar equation can be derived for the parallel CTI derived from CS4 and CS2.

Likewise, the serial CTI can be shown to be

$$\begin{aligned} CTI_s &= 1 - \left(\frac{D_4}{D_3}\right)^{1/(X_4 - X_3)} \quad \text{(A.9)} \\ &= \frac{D_3 - D_4}{D_3(X_4 - X_3)} \quad \text{(A.10)} \end{aligned}$$

A.4 Gain

We can obtain the gain A' from CS3, which is the corner source closest to the output amplifier,

$$A' = \frac{E_{^{55}\mathrm{Fe}}}{D_3}(1 - CTI_{p,i})^{Y_3}(1 - CTI_s)^{X_3} \quad \text{(A.11)}$$

where $E_{^{55}\mathrm{Fe}} = 5895.45\,\mathrm{eV}$, $X_3 = 40$ and $Y_3 = 35$. Note the term $(1 - CTI_{p,i})^{Y_3}(1 - CTI_s)^{X_3}$ which provides a small correction to the simple gain estimate of $E_{^{55}\mathrm{Fe}}/D_3$ and ensures the event energy is calculated relative to the origin $(0, 0)$ of the imaging section of the CCD.

A.5 Comparison with the CALDB gain file

The CALDB gain file defines the PHA channel to PI channel conversion as

$$PI \times G = PHA\,(GC0 + X \times GC1 + Y \times GC2) + GC3 + X \times GC4 + Y \times GC5 \qquad \text{(A.12)}$$

where GCn are the gain file coefficients (which are interpolated over time and CCD temperature), and $G = 10\,\mathrm{eV}$ is the nominal gain.

Equation A.4 can be rearranged to give the event energy from the measured DN value, assuming the CTI coefficients are known,

$$E = A'\,D\,(1 - CTI_{p,i})^{-Y}\,(1 - CTI_s)^{-X}. \qquad \text{(A.13)}$$

Note, this is the exact form of the equation required to reconstruct the event energy from the measure DN value, knowing the gain (A') and CTI values.

This equation can be made to resemble the CALDB formula by using the small value approximation expansion :

$$\begin{aligned} E &= A'\,D\,(1 + Y\,CTI_{p,i})\,(1 + X\,CTI_s) \\ &= A'\,D\,(1 + X\,CTI_s + Y\,CTI_{p,i} + X\,Y\,CTI_s\,CTI_{p,i}) \end{aligned}$$

and dropping the last term to give

$$\begin{aligned} E &= A'\,D\,(1 + X\,CTI_s + Y\,CTI_{p,i}) \\ &= D\,\{A' + X\,(A'\,CTI_s) + Y\,(A'\,CTI_{p,i})\}. \end{aligned} \qquad \text{(A.14)}$$

By comparison with equation A.12, we see that

$$\begin{aligned} GC0 &= A' \\ GC1 &= A'\,CTI_s \\ GC2 &= A'\,CTI_{p,i} \end{aligned}$$

In practise, CTI_s is estimated from corner sources CS3–CS4, while $CTI_{p,i}$ is estimated as the average parallel CTI from corner sources CS1–CS3 and CS2–CS4.

The term $GC3$ in equation A.12 represents an offset (in eV) associated with the readout electronics.

B Previous Releases

Table B.1: Previous gain file releases.

FILENAME	VALID DATE	RELEASE DATE	REVISION
swxpcgain20010101v003.fits	01-Jan-2001	15-Oct-2004	003
swxpdgain20010101v003.fits	01-Jan-2001	15-Oct-2004	003
swxwtgain20010101v003.fits	01-Jan-2001	15-Oct-2004	003
swxpcgain20010101v004.fits	01-Jan-2001	10-Jan-2005	004
swxpdgain20010101v004.fits	01-Jan-2001	10-Jan-2005	004
swxwtgain20010101v004.fits	01-Jan-2001	10-Jan-2005	004
swxpcgain20010101v005.fits	01-Jan-2001	12-Oct-2005	005
swxpdgain20010101v005.fits	01-Jan-2001	12-Oct-2005	005
swxwtgain20010101v005.fits	01-Jan-2001	12-Oct-2005	005
swxpcgain20010101v006.fits	01-Jan-2001	1-Dec-2005	006
swxpdgain20010101v006.fits	01-Jan-2001	1-Dec-2005	006
swxwtgain20010101v006.fits	01-Jan-2001	1-Dec-2005	006
swxpcgains0_20010101v007.fits	01-Jan-2001	30-Jul-2007	007
swxpcgains6_20010101v007.fits	01-Jan-2001	30-Jul-2007	007
swxpdgains0_20010101v007.fits	01-Jan-2001	30-Jul-2007	007
swxwtgains0_20010101v007.fits	01-Jan-2001	30-Jul-2007	007
swxwtgains6_20010101v007.fits	01-Jan-2001	30-Jul-2007	007
swxwtgains0_20010101v008.fits	01-Jan-2001	21-Apr-2008	008
swxwtgains6_20010101v008.fits	01-Jan-2001	21-Apr-2008	008

Table B.1 lists the gain files made available through previous releases of the *Swift*-XRT CALDB and are described in CALDB documents SWIFT-XRT-CALDB-04_v8, SWIFT-XRT-CALDB-04_v2 and SWIFT-XRT-CALDB-04.